0026-895X/11/8005-859–869$25.00
MOLECULAR PHARMACOLOGY
Copyright © 2011 The American Society for Pharmacology and Experimental Therapeutics
Mol Pharmacol 80:859–869, 2011

Vol. 80, No. 5
72769/3721862
Printed in U.S.A.

Rimonabant, a Cannabinoid Receptor Type 1 Inverse Agonist, Inhibits Hepatocyte Lipogenesis by Activating Liver Kinase B1 and AMP-Activated Protein Kinase Axis Downstream of $G\alpha_{i/o}$ Inhibition

Hong Min Wu, Yoon Mee Yang, and Sang Geon Kim

Innovative Drug Research Center for Metabolic and Inflammatory Diseases, College of Pharmacy and Research Institute of Pharmaceutical Sciences, Seoul National University, Seoul, Korea

Received April 6, 2011; accepted July 27, 2011

ABSTRACT

Liver X receptor-α (LXRα) and its target sterol regulatory element-binding protein-1c (SREBP-1c) play key roles in hepatic lipogenesis. Rimonabant, an inverse agonist of cannabinoid receptor type 1 (CB1), has been studied as an antiobesity drug. In view of the link between CB1 and energy metabolism, this study investigated the effect of rimonabant on LXRα-mediated lipogenesis in hepatocytes and the underlying basis. Rimonabant treatment inhibited CYP7A1-LXRα response element gene transactivation and an increase in LXRα mRNA level by the LXRα agonist *N*-(2,2,2-trifluoroethyl)-*N*-[4-[2,2,2-trifluoro-1-hydroxy-1-(trifluoromethyl) ethyl]phenyl]-benzenesulfonamide (T0901317) in HepG2 cells. Rimonabant consistently attenuated the activation of SREBP-1c and its target gene induction. The reversal by CB1 agonists on rimonabant's repression of SREBP-1c supported the role of CB1 in this effect. Rimonabant inhibited the activation of SREBP-1c presumably via $G\alpha_{i/o}$ inhibition, as did pertussis toxin. Adenylyl cyclase activator forskolin or 8-bromo-cAMP treatment mimicked the action of rimonabant, suggesting that $G\alpha_{i/o}$ inhibition causes repression of SREBP-1c by increasing the cAMP level. Knockdown or chemical inhibition of protein kinase A (PKA) prevented the inhibition of LXRα by rimonabant, supporting the fact that an increase in cAMP content and PKA activation, which catalyzes LXRα inhibitory phosphorylation, might be responsible for the antilipogenic effect. In addition, rimonabant activated liver kinase B1 (LKB1), resulting in the activation of AMP-activated protein kinase responsible for LXRα repression. Moreover, PKA inhibition prevented the activation of LKB1, supporting the fact that PKA regulates LKB1. In conclusion, rimonabant has an antilipogenic effect in hepatocytes by inhibiting LXRα-dependent SREBP-1c induction, as mediated by an increase in PKA activity and PKA-mediated LKB1 activation downstream of CB1-coupled $G\alpha_{i/o}$ inhibition.

Introduction

The metabolic syndrome is made up of a series of obesity- and heart disease-related risk factors including hypertension, hyperglycemia, and dyslipidemia (Cornier et al., 2008). The increasing rate of obese subjects in the world results in the growing incidence of metabolic syndrome (Alexander et al., 2003). Mechanisms of the pathogenesis involved in the disorders are not yet fully understood. Nonalcoholic fatty liver disease, a hepatic component of metabolic syndrome, is a common liver disease that refers to liver dysfunction and/or injury, disturbing the overall metabolic function of the liver (Kotronen and Yki-Järvinen, 2008). Nonalcoholic fatty liver disease ranges

This work was supported by the National Research Foundation of Korea funded by the Korean Ministry of Education, Science and Technology Development [Grant 2011-0001204].
H.M.W. and Y.M.Y. contributed equally to this work.
Article, publication date, and citation information can be found at http://molpharm.aspetjournals.org.
doi:10.1124/mol.111.072769.

ABBREVIATIONS: LXRα, liver X receptor-α; T090, T0901317, *N*-(2,2,2-trifluoroethyl)-*N*-[4-[2,2,2-trifluoro-1-hydroxy-1-(trifluoromethyl)ethyl]phenyl]-benzenesulfonamide; LXRE, LXRα-response element; SREBP-1c, sterol regulatory element binding protein-1c; FAS, fatty acid synthase; ACC, acetyl-CoA carboxylase; SCD-1, stearoyl-CoA desaturase-1; ABCA1, ATP-binding cassette transporter A1; CB1, cannabinoid receptor type 1; AMPK, AMP-activated protein kinase; PKA, cAMP-dependent protein kinase A; LKB1, liver kinase B1; Hu 210, (6*aR*)-*trans*-3-(1,1-dimethylheptyl)-6*a*,7,10,10*a*-tetrahydro-1-hydroxy-6,6-dimethyl-6*H*-dibenzo[*b,d*]pyran-9-methanol; ACEA, arachidonyl-2′-chloroethylamide; PKI, PKA inhibitor; CaMKK, calcium/calmodulin-dependent kinase kinase; GW3965 3-[3-[*N*-(2-chloro-3-trifluoromethylbenzyl)-(2,2-diphenylethyl)amino]propyloxy]phenylacetic acid hydrochloride; 8-Br-cAMP, 8-bromo-cAMP; H89, *N*-[2-(*p*-bromocinnamylamino)ethyl]-5-isoquinolinesulfonamide; PCR, polymerase chain reaction; GAPDH, glyceraldehyde-3-phosphate dehydrogenase; siRNA, small interfering RNA; PXRE, pregnane X receptor response element; AM251, *N*-(piperidin-1-yl)-5-(4-iodophenyl)-1-(2,4-dichlorophenyl)-4-methyl-1*H*-pyrazole-3 carboxamide; GPCR, G protein-coupled receptor; CAB39, calcium binding protein 39; STO-609, 7*H*-benz[de]benzimidazo[2,1-*a*]isoquinoline-7-one-3-carboxylic acid acetate; DN, dominant-negative; S6K1, p70 ribosomal S6 kinase-1.

from steatosis to steatohepatitis, fibrosis, and cirrhosis (Marra et al., 2008).

Liver X receptor-α (LXRα), a lipid sensor, promotes lipid and cholesterol metabolism in the cell. In regulating lipid metabolism, LXRα stimulates fatty acid synthesis and triglyceride accumulation in hepatocytes. Upon activation with LXR ligand [e.g., endogenous ligand, oxysterol, and synthetic ligand, *N*-(2,2,2-trifluoroethyl)-*N*-[4-[2,2,2-trifluoro-1-hydroxy-1-(trifluoromethyl)ethyl]phenyl]-benzenesulfonamide (T0901317; T090)], LXRα, and retinoid X receptor dimerize and bind to LXRα response elements (LXRE). Sterol regulatory element-binding protein (SREBP)-1c is a major target gene of LXRα (Repa et al., 2000) and plays a key role in the induction of lipogenic genes such as fatty acid synthase (FAS), acetyl-CoA carboxylase (ACC), stearoyl-CoA desaturase-1 (SCD-1), and ATP-binding cassette (ABC) transporter A1 (Ntambi, 1999; Stoeckman and Towle, 2002). Thus, SREBP-1c activation by LXRα may facilitate progression to steatosis and steatohepatitis (Repa et al., 2000). Therefore, methods to inhibit LXRα activity represent a potential way for the treatment of hepatic steatosis.

Cannabinoid receptor type 1 (CB1) has a modulating effect on the fat metabolism at peripheral organs such as liver, adipose tissue, and skeletal muscle (Liu et al., 2005; Osei-Hyiaman et al., 2005; Yan et al., 2007). In several animal models, CB1 blockade decreases de novo lipogenesis (Jeong et al., 2008; Jourdan et al., 2010). Rimonabant (SR141716A) is the first-in-class CB1 blocker for obesity treatment (Van Gaal et al., 2005). The data obtained from clinical trials suggest that rimonabant may have a beneficial effect against disrupted lipid metabolism in the liver (Després et al., 2005; Scheen et al., 2006; Hollander et al., 2010). However, the antisteatotic effect of rimonabant in hepatocytes and the molecular basis responsible for this action remain to be elucidated.

Protein kinase A (PKA), recognized as a fasting signal that is sensitive to increased cAMP content, plays a role in lipid metabolism (McKnight et al., 1998). In animal models, PKA activation by adrenergic stimulation resulted in lean phenotypes and improves insulin sensitivity (Cummings et al., 1996; Schreyer et al., 2001). In addition, PKA directly phosphorylates LXRα and thereby hinders LXRα dimerization with retinoid X receptor (Yamamoto et al., 2007). Thus, PKA activation attenuates SREBP-1 activity and SREBP-1-mediated lipogenesis (Lu and Shyy, 2006; Yamamoto et al., 2007). Because CB1 is coupled to G proteins, chemical modulation of this receptor may affect the adenylyl cyclase-cAMP-dependent PKA axis (Bayewitch et al., 1995).

AMP-activated protein kinase (AMPK) serves as an intracellular sensor for energy homeostasis. The AMPK pathway regulates lipid and glucose metabolism; its activation inhibits not only hepatic lipogenesis mainly through inhibitory phosphorylation of ACC, a rate-limiting step of fatty acid synthesis, but also hepatic cholesterol production through suppression of 3-HMG-CoA reductase (Motoshima et al., 2006). In addition, an increase in AMPK activity reduces glucose production in the liver, whereas it enhances glucose uptake in the skeletal muscle (Sakoda et al., 2002). A series of findings indicate that AMPK contributes to antisteatotic and antidiabetic action (Bae et al., 2007; Hwahng et al., 2009). In hepatic and adipose tissues, CB1 agonist treatment has been shown to inhibit AMPK activity (Kola et al., 2005). Thus, it is plausible that the antagonism of CB1 may result in the activation of AMPK.

In view of the association between endocannabinoid physiology and lipid metabolism and the inhibitory regulation of AMPK by CB1, we were interested in the effect of rimonabant, a selective CB1 inverse agonist, on LXRα-SREBP-1c-mediated lipogenesis in hepatocytes and the underlying basis. Here, we report the beneficial effect of rimonabant's antagonism of CB1 on LXRα-SREBP-1c-mediated lipogenesis. Moreover, this study identified the regulatory role of PKA in activating liver kinase B1 (LKB1) and AMPK downstream of CB1 inverse agonism. An important finding of this study is the link between CB1-G$\alpha_{i/o}$ inhibition and LKB1-AMPK activation that leads to the inhibition of LXRα-mediated-SREBP-1c activity.

Materials and Methods

Materials. Rimonabant HCl (99%) was provided from AK Scientific (Mountain View, CA). (6a*R*)-*trans*-3-(1,1-Dimethylheptyl)-6a,7,10,10a-tetrahydro-1-hydroxy-6,6-dimethyl-6*H*-dibenzo[*b,d*]pyran-9-methanol (Hu 210) and arachidonyl-2′-chloroethylamide (ACEA) were purchased from Tocris Bioscience (Ellisville, Missouri). Anti-phospho-AMPK, anti-AMPK, anti-phospho-ACC, anti-ACC, anti-acetylated lysine, and anti-phospho-LKB1 (Ser428) antibodies were obtained from Cell Signaling Technology (Danvers, MA). PKI (a PKA inhibitor) and the antibodies directed against SREBP-1, Gα_i, PKA, LKB1, c-myc, and calcium/calmodulin-dependent kinase kinase (CaMKK) β were supplied from Santa Cruz Biotechnology, Inc. (Santa Cruz, CA). Anti-β-actin and anti-phosphorylated serine antibody, 3-[3-[*N*-(2-chloro-3-trifluoromethylbenzyl)-(2,2-diphenylethyl)amino]propyloxy] phenylacetic acid hydrochloride (GW3965), 8-Br-cAMP, and forskolin were obtained from Sigma-Aldrich Co. (St. Louis, MO). Horseradish peroxidase-conjugated goat anti-rabbit and goat anti-mouse IgGs were purchased from Zymed Laboratories (South San Francisco, CA). Pertussis toxin, *N*-[2-(*p*-bromocinnamylamino) ethyl]-5-isoquinolinesulfonamide (H89), T0901317, and compound C were obtained from Calbiochem (San Diego, CA).

Cell Culture. HepG2 (human hepatocyte-derived cell line), AML-12 (mouse hepatocyte-derived cell line), and HeLa cells were supplied from American Type Culture Collection (Manassas, VA). All cells were maintained in Dulbecco's modified Eagle's medium supplemented with 10% fetal bovine serum, 50 units/ml penicillin, and 50 μg/ml streptomycin at 37°C in a humidified atmosphere with 5% CO_2. Cells were plated in a six-well dish at a density of 10^6 cells/well, and wells with 70 to 80% confluence were used. The cells were incubated with either vehicle or LXRα agonist (i.e., T090 and GW3965) in combination with rimonabant for 12 h.

Transient Transfection and Reporter Gene Assays. The cells were transiently transfected with pGL2-FAS (1 μg) or TK-CYP7A1-LXREx3-LUC (0.5 μg) for 3 h in the presence of Lipofectamine 2000 reagent. The activity of luciferase was measured by adding luciferase assay reagent (Promega, Madison, WI). The FAS reporter plasmid (pGL2-FAS) was a gift from Dr. T. F. Osborne (University of California, Irvine, CA). LXR luciferase reporter TK-CYP7a-LXREx3-LUC, which contains three tandem copies of the sequence (5′-gcttTGGTCActcaAGTTCAagtta-3′) from the rat *CYP7A1* gene, was provided from Dr. D. J. Mangelsdorf (University of Texas Southwestern Medical Center, Dallas, TX).

RNA Isolation and Real-Time PCR Assays. Total RNA was extracted using TRIzol (Invitrogen, Carlsbad, CA) according to the manufacturer's instructions. cDNA was obtained by reverse transcription using an oligo$(dT)_{16}$ primer. It was amplified by PCR. Real-time PCR was conducted with a LightCycler 1.5 apparatus (Roche, Mannheim, Germany) using a LightCycler DNA Master SYBR Green I kit

according to the manufacturer's instructions. The levels of target mRNAs were normalized to those of glyceraldehyde-3-phosphate dehydrogenase (GAPDH) mRNA. The following primer sequences were used: human SREBP-1, 5′-CGACATCGAAGACATGCTTCAG-3′ (sense) and 5′-GGAAGGCTTCAAGAGAGGAGC-3′ (antisense); human LXRα, 5′-GATCGAGGTGATGCTTCTGGAG-3′ (sense) and 5′-CCCTGCTTTGGCAAAGTCTTC-3′ (antisense); human FAS, 5′-GACATCGTCCATTCGTTTGTG-3′ (sense) and 5′-CGGATCACCTTCTTGAGCTCC-3′ (antisense); human ACC1, 5′-GCTGCTCGGATCACTAGTGAA-3′ (sense) and 5′-TTCTGCTATCAGTCTGTCCAG-3′ (antisense); human SCD-1, 5′-CCTCTACTTGGAAGACGACATTCGC-3′ (sense) and 5′-GCAGCCGAGCTTTGTAAGAGCGGT-3′ (antisense); human ABCA1, 5′-TGTCCAGTCCAGTAATGGTTCTGT-3′ (sense) and 5′-AAGCGAGATATGGTCCGGATT-3′ (antisense); and human GAPDH, 5′-GAAGATGGTGATGGGATTTC-3′ (sense) and 5′-GAAGGTGAAGGTCGGAGTC-3′ (antisense).

Immunoprecipitation and Immunoblot Assays. Cell lysates (500 μg/each aliquot) were immunoprecipitated with anti-LXRα antibody or anti-LKB1 antibody overnight at 4°C. The antigen-antibody complex was immunoprecipitated after incubation with protein G-agarose for 2 h. Immune complexes were solubilized in 2× Laemmli buffer and were boiled for 5 min. Protein samples were resolved and were immunoblotted with anti-phosphorylated serine, anti-phosphorylated threonine, or anti-acetylated lysine antibody.

siRNA Knockdown. To knock down target molecules, cells were transfected with either an siRNA directed against human Gα_i, PKA, or LKB1 (Santa Cruz Biotechnology, Inc.) or a nontargeting control siRNA (100 pmol/ml) using Lipofectamine 2000 according to the manufacturer's instructions. After transfection for 48 h, the cells were treated with vehicle or LXRα agonist in the presence or absence of rimonabant for 12 h. Immunoblotting verified the knockdown effects of Gα_i, PKA, and LKB1.

PKA Activity Assay. The PKA assay was performed using a commercially available solid-phase enzyme-linked immunosorbent assay kit (Enzo Life Sciences, Farmingdale, NY), according to the manufacturer's instruction. In brief, samples (30 μg each) were loaded in the appropriate wells of the PKA substrate microtiter plate, followed by addition of 10 μg of ATP. After termination of the kinase reaction, the antibody that recognizes the substrate phosphorylation was added to the wells. The phosphospecific antibody was then bound by a peroxidase-conjugated secondary antibody. The color of the assay was developed in proportion to PKA phosphotransferase activity using tetramethylbenzidine substrate. After color development was stopped with acid stop solution, the intensity of the color was measured in a microplate reader (Tecan, Durham, NC) at 450 nm.

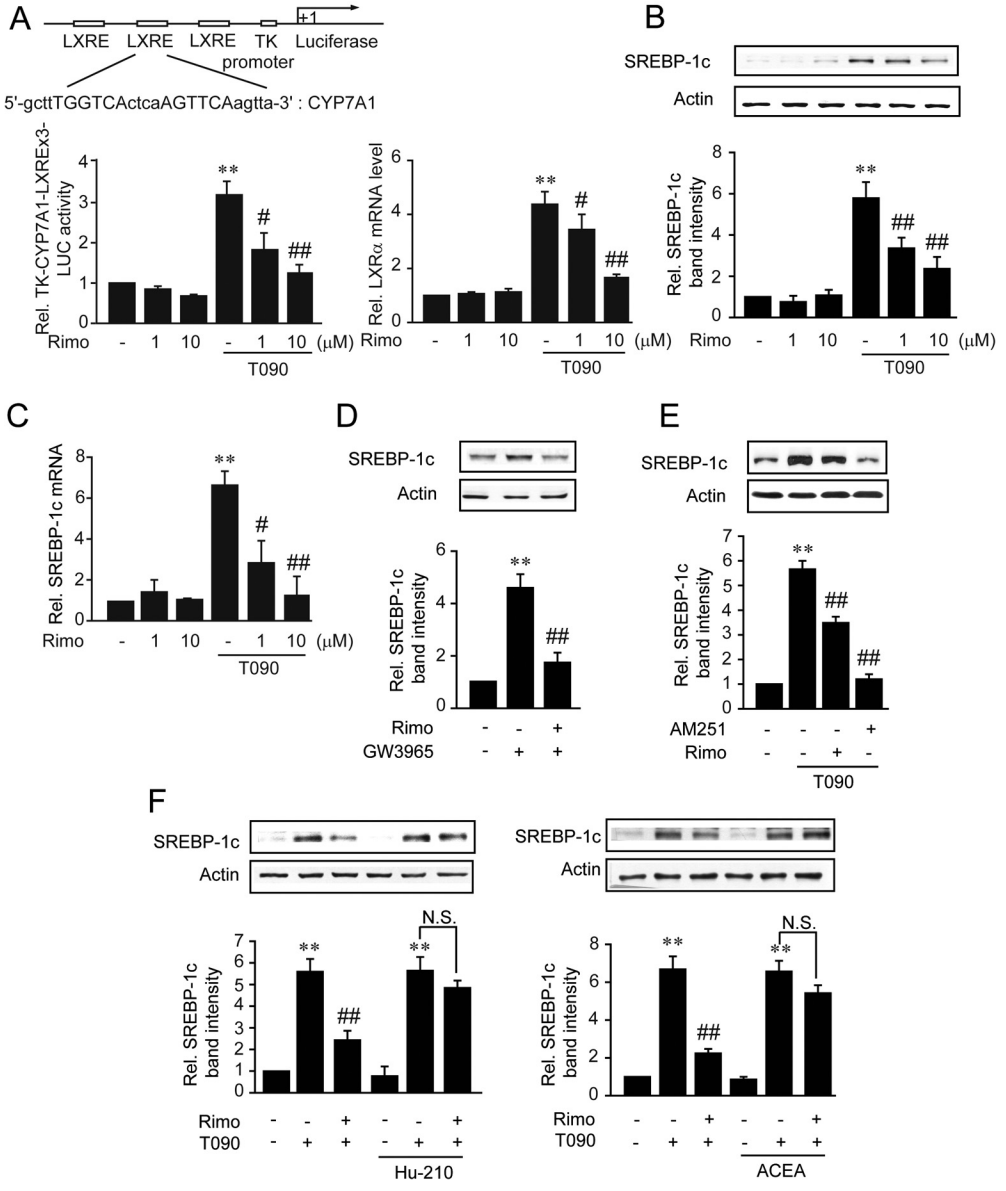

Fig. 1. Effect of rimonabant (Rimo) on LXRα and SREBP-1c activation. A, inhibition of LXRα activity. The relative (Rel.) LXRE luciferase (LUC) activity (left) was measured on the lysates of HepG2 cells transfected with an LXRE-luciferase construct and treated with different treatment combinations (vehicle or 1 or 10 μM rimonabant for 13 h; 1 μM T090 for 12 h). LXRα transcript levels were analyzed using real-time PCR assays (right). B, SREBP-1c repression by rimonabant. SREBP-1c was assessed by immunoblotting. C, real-time PCR assays for SREBP-1c mRNA. D, rimonabant inhibition of SREBP-1c induction by GW3965. SREBP-1c was immunoblotted in the lysates of cells treated with 10 μM rimonabant for 1 h and continuously exposed to 5 μM GW3965 for 12 h. E, SREBP-1c repression by AM251. Cells were treated with 1 μM rimonabant or 1 μM AM251 for 1 h and continuously exposed to 1 μM T090 for 12 h. F, reversal by CB1 agonists of rimonabant's repression of SREBP-1c. HepG2 cells were treated with 100 nM Hu 210 or 10 nM ACEA for 1 h and subjected to different treatment combinations. Data represent the mean ± S.E. for at least three separate experiments. For LXRE luciferase activity assay and all immunoblots, the statistical significance of differences between each treatment group and control (**, $p < 0.01$) or T090 or GW3965 alone (#, $p < 0.05$; ##, $p < 0.01$) was determined. For all real-time PCR assays, the mRNA level of GAPDH was used as a reference for data normalization. Fold changes were calculated by correlation coefficients of crossing point for triplicate PCR results. Statistical significance of differences between each treatment group and the control (**, $p < 0.01$) or T090 alone (#, $p < 0.05$; ##, $p < 0.01$) was determined. N.S., not significant.

Data Analysis. One-way analysis of variance procedures were used to assess significant differences among treatment groups. For each significant treatment effect, the Newman-Keuls test was used to compare multiple group means.

Results

Inhibition of LXRα-Dependent SREBP-1c Induction. The in vitro effect of rimonabant on lipogenic gene induction by T090 was examined in HepG2 cells: T090, a synthetic LXRα agonist, was used to induce LXRα and SREBP-1c activation. Treatment of cells with T090 increased LXR-dependent gene transactivation, as shown by an increase in CYP7A1-LXRE-luciferase (CYP7A1) activity, which was significantly attenuated by simultaneous treatment of cells with rimonabant (Fig. 1A, left). T090 may also increase transactivation of the pregnane X receptor target gene (CYP3A23-PXRE-luciferase gene) (Mitro et al., 2007). PXRE reporter activity was unaffected by rimonabant (data not shown), confirming that rimonabant treatment specifically inhibits the induction of the LXRα target gene. Because the LXRα gene itself contains an LXRE (Laffitte et al., 2001), the activation of LXRα by T090 treatment for 12 h caused its own gene induction. This increase was prevented by concomitant treatment of cells with rimonabant (Fig. 1A, right).

The effect of rimonabant on T090-dependent induction of SREBP-1c, a marker of hepatic lipogenesis, was determined in HepG2 cells. As expected, the level of SREBP-1c protein was increased 12 h after T090 treatment, and rimonabant attenuated the T090 induction of SREBP-1c protein (Fig. 1B): the SREBP-1c transcript level was also repressed by 1 or 10 μM rimonabant pretreatment (Fig. 1C). Moreover, treatment of cells with rimonabant prevented the ability of GW3965, another LXRα agonist, to induce SREBP-1c expression (Fig. 1D). *N*-(Piperidin-1-yl)-5-(4-iodophenyl)-1-(2,4-dichlorophenyl)-4-methyl-1*H*-pyrazole-3 carboxamide (AM251), a CB1 antagonist, blocked SREBP-1c induction by T090, as did rimonabant (Fig. 1E). In addition, treatment of cells with Hu 210 or ACEA, CB1 agonists, reversed the ability of rimonabant to inhibit SREBP-1c induction by T090 (Fig. 1F). Our results indicate that rimonabant antagonizes the activation of LXRα and SREBP-1c by T090, which may be mediated by CB1 antagonism.

Inhibition of SREBP-1c-Mediated Lipogenic Gene Induction. To assess the transcriptional activity of SREBP-1c, FAS reporter assays were conducted in HepG2 cells transfected with the construct containing the sterol response element, but not the LXRE, in the −150-base pair FAS promoter region (Fig. 2A, upper). Incubation of the

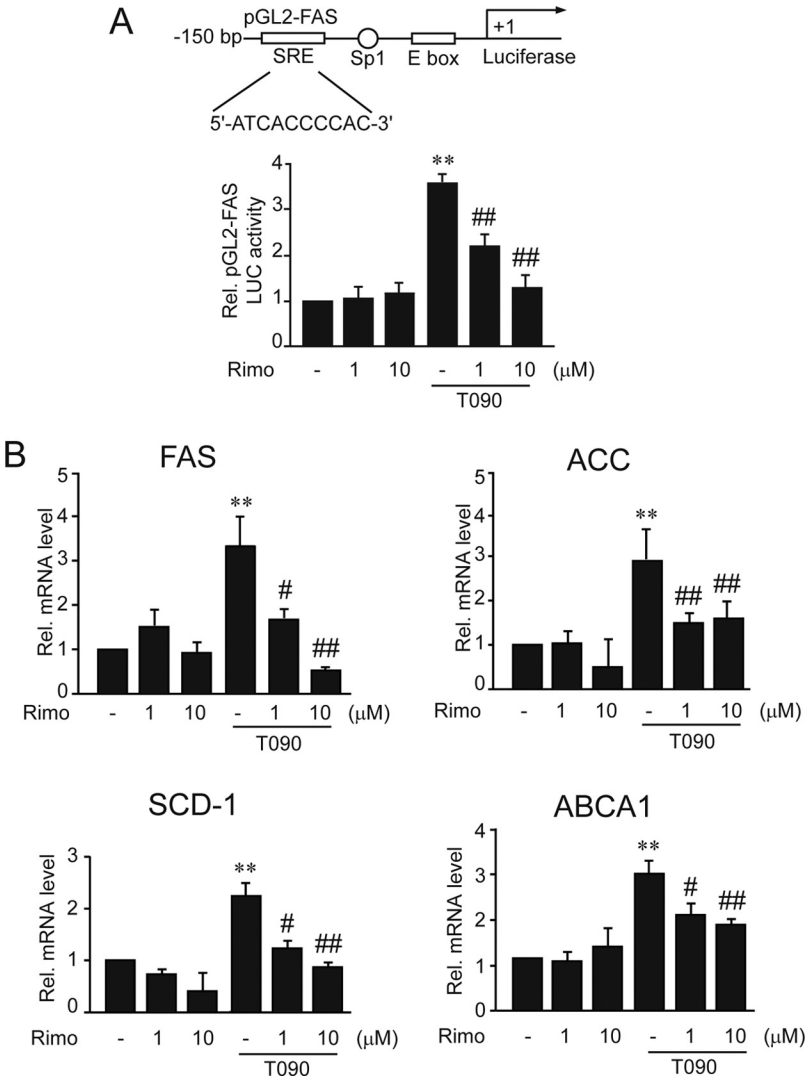

Fig. 2. Inhibition of SREBP-1c target gene induction by rimonabant (Rimo). A, rimonabant inhibition of FAS gene transactivation. FAS luciferase (LUC) assays were performed on the lysates of HepG2 cells subjected to various treatment combinations (vehicle, 1 μM or 10 μM rimonabant for 13 h. and/or 1 μM T090 for 12 h). B, real-time PCR assays. The transcripts of lipogenic genes were analyzed by real-time PCR assays, with the mRNA level of GAPDH used as a reference for data normalization. Data represent the means ± S.E. of four separate experiments. For both A and B, statistical significance of differences between each treatment group and the control (**, $p < 0.01$) or T090 alone (#, $p < 0.05$; ##, $p < 0.01$) was determined. bp, base pairs; Rel., relative.

cells with T090 increased luciferase activity from the construct, which was diminished by rimonabant (Fig. 2A, lower). Because SREBP-1c controls the transcription of genes encoding for lipogenic enzymes, the effects of rimonabant on their gene expression were monitored by measuring relative changes in FAS, ACC, SCD-1, and ABCA1 transcript levels (Fig. 2B). Rimonabant attenuated the ability of LXRα agonist to induce the target genes of SREBP-1c. Our results demonstrate that rimonabant indeed has the ability to prevent SREBP-1c-mediated lipogenic gene induction by LXRα agonist. In subsequent experiments, 10 μM rimonabant was used to ensure the optimal effect.

SREBP-1c Repression by cAMP-PKA Activation Downstream of G$\alpha_{i/o}$ Inhibition. GPCRs that activate the Gα_i class of Gα subunits inhibit cAMP production, whereas other GPCRs that activate the Gα_s class of Gα subunits facilitate it (Neves et al., 2002). CB1 may be coupled with G proteins of the G$\alpha_{i/o}$ family (i.e., Gα_i 1, 2, and 3 and Gα_o 1 and 2), triggering signaling pathways mainly by inhibiting the cAMP-dependent PKA pathway. As an effort to identify the downstream component of CB1 antagonism, we examined the role of G$\alpha_{i/o}$ inhibition in the repression of lipogenesis by rimonabant. Either knockdown of Gα_i or treatment of cells with pertussis toxin (a G$\alpha_{i/o}$ inhibitor) inhibited T090-mediated induction of SREBP-1c (Fig. 3A). G$\alpha_{i/o}$ inhibition causes an increase in cellular cAMP content through adenylyl cyclase (Neves et al., 2002). Treatment of cells with forskolin, an agent that increases cAMP by activating adenylyl cyclase, also inhibited the induction of SREBP-1c by T090 (Fig. 3B, left). Likewise, 8-Br-cAMP treatment diminished SREBP-1c induction by T090 (Fig. 3B, right). Because cAMP activates PKA, we next assessed the effect of rimonabant on the activity of PKA. As expected, rimonabant elevated PKA activity, which was abolished by treatment of cells with either H89 (a PKA/PKG/PKC inhibitor) or PKI (a PKA-specific inhibitor) (Fig. 3C).

Role of PKA in the Inhibition of LXRα and SREBP-1c Activation. PKA may directly phosphorylate LXRα at the serine residue, which inactivates LXRα (Yamamoto et al., 2007). Consistent with this report, rimonabant facilitated the phosphorylation of LXRα at the serine residue, which was reversed by either PKA knockdown (PKA siRNA) or H89

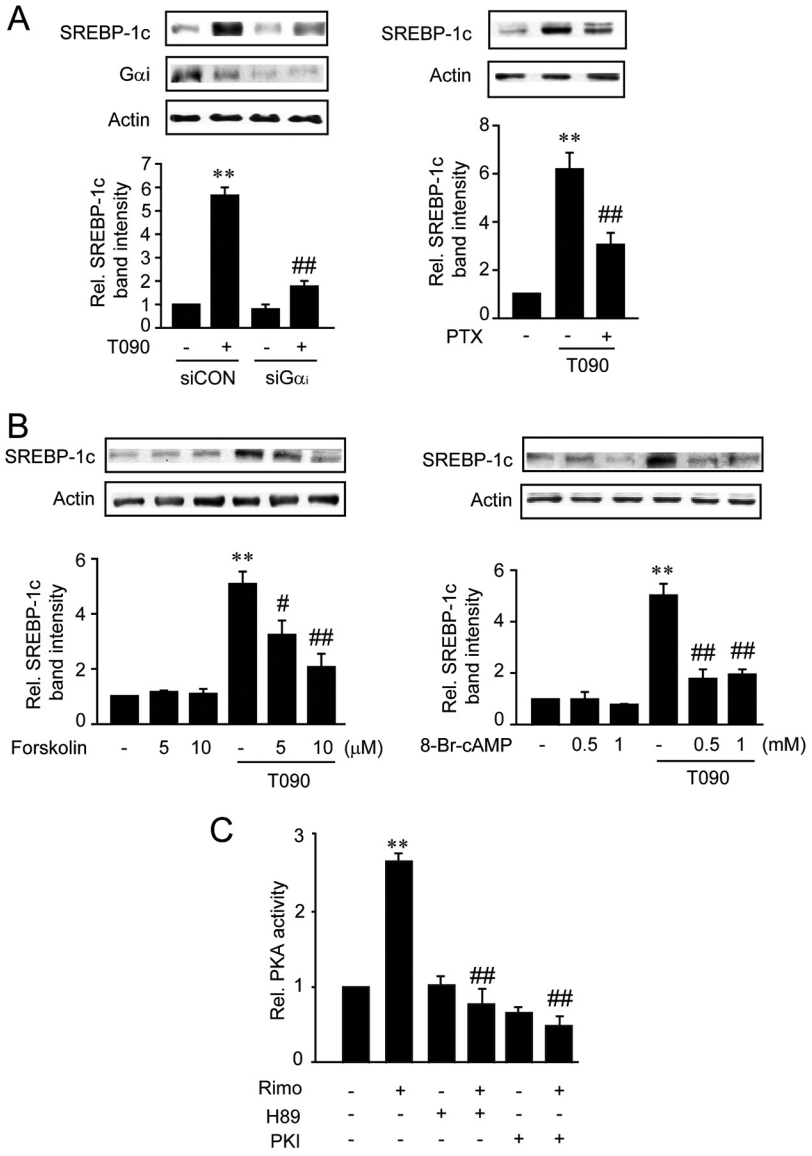

Fig. 3. Role of the G$\alpha_{i/o}$-cAMP-PKA axis in SREBP-1c repression by rimonabant (Rimo). A, effect of G$\alpha_{i/o}$ inhibition on SREBP-1c expression. HepG2 cells were treated with 1 μM T090 for 12 h after Gα_i siRNA transfection (100 pmol/ml) for 48 h (left) or 100 ng/ml pertussis toxin (PTX) treatment for 1 h (right). SREBP-1c was immunoblotted on the cell lysates. B, SREBP-1c repression by cAMP. Cells were treated with 1 μM T090 after incubation with forskolin or 8-Br-cAMP for 1 h. C, effect of rimonabant on PKA activity. PKA activity was determined 30 min after treatment of cells with 10 μM rimonabant, rimonabant plus H89 (1 μM, 30-min pretreatment), or rimonabant plus PKI (10 μM, 30-min pretreatment). Data represent the mean $\pm$ S.E. for at least three separate experiments. For both A and B, statistical significance of differences between each treatment group and the control (**, $p < 0.01$) or T090 alone (#, $p < 0.05$; ##, $p < 0.01$) was determined. For PKA activity assay, statistical significance of differences between each treatment group and the control (**, $p < 0.01$) or rimonabant alone (##, $p < 0.01$) was determined. Rel., relative; siCON, control siRNA; siGα_i, Gα_i siRNA.

treatment (Fig. 4A). Furthermore, H89 attenuated the ability of rimonabant to prevent LXRE reporter induction by T090 (Fig. 4B). Moreover, either transfection of specific siRNA directly against the PKA α catalytic subunit or H89 treatment reversed the repression of SREBP-1c by rimonabant (Fig. 4C). Hence, cAMP-dependent PKA activation by rimonabant may contribute to SREBP-1c repression by rimonabant via LXRα inactivation.

PKA-Dependent Activation of LKB1 by Rimonabant. PKA may activate LKB1 through direct phosphorylation (Collins et al., 2000). Given the regulatory effect of PKA on LKB1, we next examined whether rimonabant is capable of activating LKB1. Rimonabant promoted the activation of LKB1 in HepG2 or AML-12 cells (a normal mouse hepatocyte cell line, known to synthesize fatty acids/lipids), as shown by increased phosphorylation of LKB1 on the Ser428 residue (Fig. 5A). LKB1 activation was further supported by its deacetylation and binding with calcium binding protein 39 (CAB39) (Fig. 5B). To link the increased PKA activity and LKB1 activation by rimonabant, we determined whether PKA inhibition affected LKB1 activation by rimonabant. We found that siRNA knockdown of PKA completely prevented the ability of rimonabant to promote LKB1 phosphorylation (Fig. 5C). Likewise, treatment of cells with H89 abolished the activation of LKB1 by rimonabant (Fig. 5D). These data provide evidence that the increase in PKA activity by rimonabant may lead to the activation of LKB1.

LKB1-Dependent AMPK Activation for the Inhibition of LXRα. LKB1 is an upstream kinase of AMPK. As expected, rimonabant activated AMPK in a time-dependent manner, as evidenced by phosphorylations of AMPK and ACC (a substrate of AMPK) in HepG2 or AML12 cells (Fig. 6A). siRNA knockdown of LKB1 consistently eliminated the ability of rimonabant to activate AMPK (Fig. 6B, left). In addition, rimonabant did not activate AMPK in HeLa cells deficient in LKB1 (Fig. 6B, right). CaMKKβ is a member of the serine/threonine protein kinase family. Treatment of cells with 7*H*-benz[de]benzimidazo[2,1-*a*]isoquinoline-7-one-

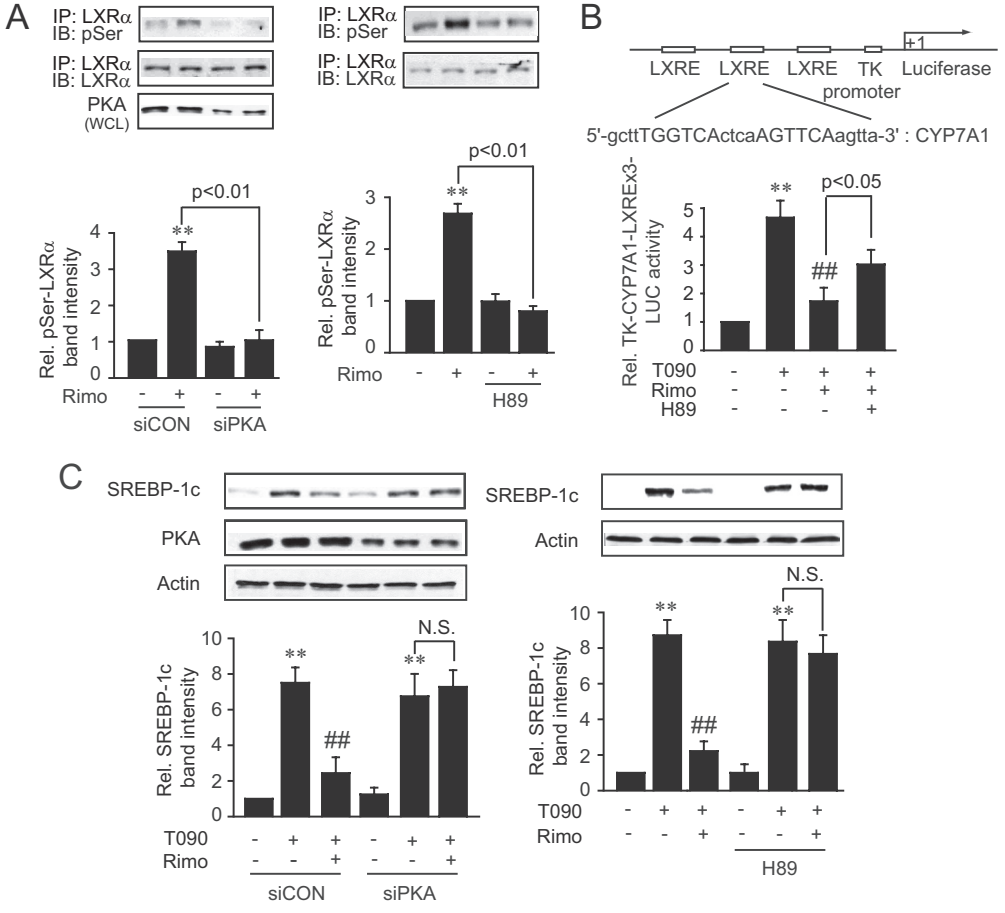

Fig. 4. Role of PKA in the repression of LXRα-SREBP-1c by rimonabant (Rimo). A, effect of PKA on serine phosphorylation of LXRα by rimonabant. HepG2 cells were treated with vehicle or 10 μM rimonabant after siPKA transfection (100 pmol/ml) for 48 h or 1 μM H89 treatment for 1 h. LXRα immunoprecipitates (IP) were immunoblotted (IB) with anti-phosphorylated serine antibody (pSer). After verifying equal loading of proteins in each experiment by immunoblotting of LXRα immunoprecipitates for LXRα, the relative protein levels of pSer-LXRα from at least three separate experiments were compared among four treatment groups in each experimental set (i.e., siCON + vehicle, siCON + rimonabant, siPKA + vehicle, and siPKA + rimonabant; or vehicle, vehicle + rimonabant, H89 + vehicle, and H89 + rimonabant) by analysis of variance and multiple comparisons (**, $p < 0.01$; compared from siCON + vehicle or vehicle-treated group). Left LXRα control blot is also control blot for pThr-LXRα (Fig 6D, right). B, effect of PKA inhibition on LXRα repression by rimonabant. LXRE luciferase activity was measured on the lysates of HepG2 cells treated with different treatment combinations after 1 μM H89 treatment for 30 min. C, reversal by PKA inhibition of rimonabant repression of SREBP-1c. Immunoblots were performed on the lysates of cells treated with 1 μM T090 or 1 μM T090 plus 10 μM rimonabant for 12 h after PKA knockdown (100 pmol/ml, 48 h) or H89 treatment. For B and C, data represent the mean ± S.E. for at least three separate experiments. The statistical significance of differences between each treatment group and control (**, $p < 0.01$) or T090 alone (##, $p < 0.01$) was determined. WCL, whole-cell lysate; Rel., relative; siCON, control siRNA; siPKA, PKA siRNA; N.S., not significant.

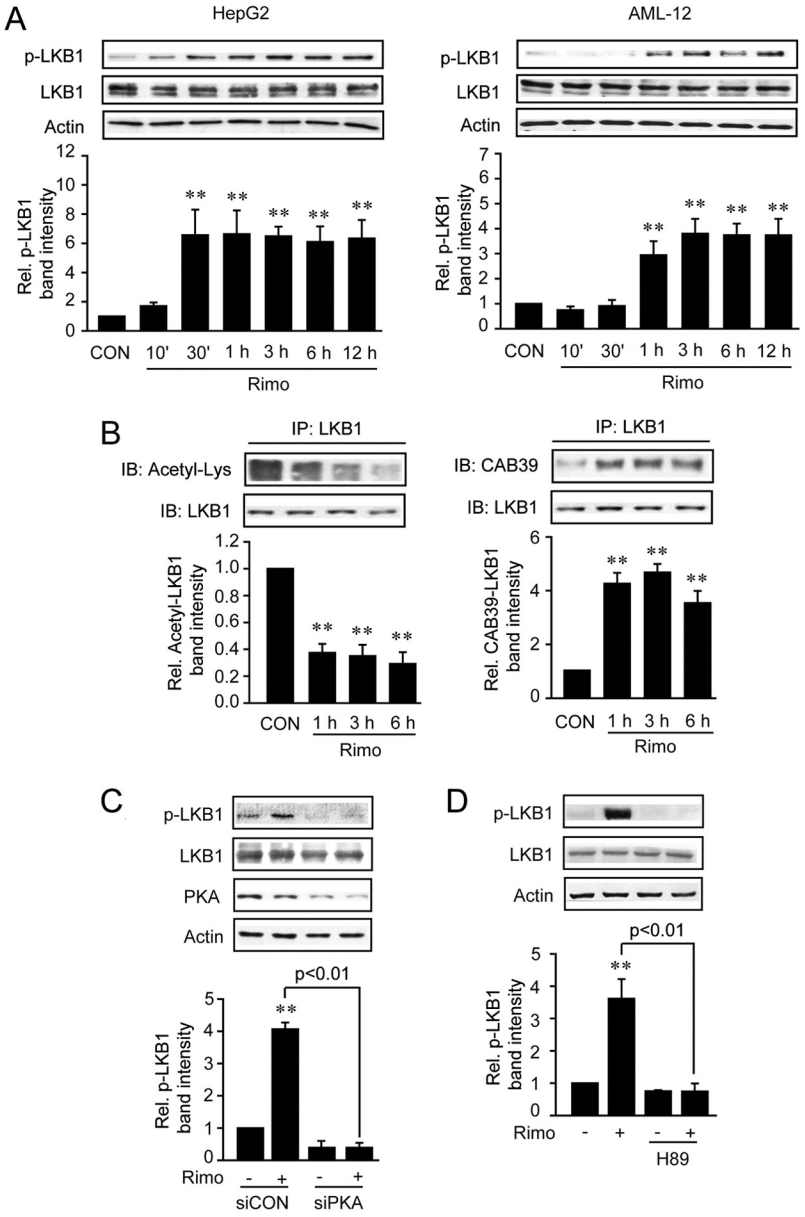

Fig. 5. Role of PKA in the activation of LKB1 by rimonabant (Rimo). A, LKB1 phosphorylation by rimonabant. Phosphorylated LKB1 (p-LKB1) or the total form of LKB1 was immunoblotted on the lysates of cells treated with 10 μM rimonabant for the indicated time periods. B, LKB1 deacetylation and binding with CAB39 by rimonabant. LKB1 immunoprecipitates (IP) were immunoblotted (IB) with either anti-acetylated-lysine antibody or anti-CAB39 antibody. C, effect of PKA knockdown on LKB1 phosphorylation. HepG2 cells were treated with 10 μM rimonabant for 3 h after siRNA knockdown (100 pmol/ml, 48 h). D, effect of H89 on LKB1 phosphorylation. Cells were treated with 1 μM H89 for 30 min and were continuously incubated with 10 μM rimonabant for 3 h. For all immunoblots, data represent the mean ± S.E. for at least three separate experiments (significant compared with control, **, $p < 0.01$). Rel., relative; CON, control; siCON, control siRNA; siPKA, PKA siRNA.

3-carboxylic acid acetate (STO-609) (1 μg/ml), an inhibitor of CaMKK, failed to antagonize AMPK activation by rimonabant (Fig. 6C). Inhibition of CaMKKβ autophosphorylation at serine/threonine by STO-609 confirmed the effectiveness of STO-609. All of these results show that rimonabant activates AMPK through LKB1 but not through CaMKKβ.

Activated AMPK inhibits LXRα through phosphorylation at the threonine residue (Hwahng et al., 2009). To verify the role of AMPK in repressing LXRα and SREBP-1c by rimonabant, we assessed the effect of AMPK inhibition on the ability of rimonabant to repress T090 activation of LXRα and SREBP-1c induction. As expected, overexpression of a dominant-negative mutant of AMPKα (DN-AMPKα) reversed LXRα phosphorylation at the threonine residue increased by rimonabant (Fig. 6D, left), whereas it did not affect LXRα phosphorylation at the serine residue (Fig. 6D, middle). Because PKA is the upstream kinase of the LKB1-AMPK axis, PKA activation also leads to the phosphorylation of LXRα at threonine through AMPK (Fig., 6D, right). Because the antibodies directed against the phosphoserine or phosphothreonine of LXRα were not available, LXRα immunoprecipitates were immunoblotted for phosphoserine or phosphothreonine. AMPK inhibition consistently antagonized the ability of rimonabant to repress SREBP-1c (Fig. 6E, left). Likewise, treatment of cells with compound C, a chemical inhibitor of AMPK, reversed the SREBP-1c-repressing effect of rimonabant (Fig. 6E, right). Our results showed that AMPK activation by rimonabant contributes to repression of SREBP-1c, presumably via LXRα inhibition (i.e., threonine phosphorylation). Rimonabant has an antilipogenic effect in hepatocytes not only by promoting PKA activation, which directly inhibits LXRα, but also by PKA-mediated activation of AMPK responsible for LXRα-SREBP-1c repression (Fig. 7).

Discussion

Rimonabant is the pioneering CB1 inverse agonist that had been used in clinical settings on the basis of its body

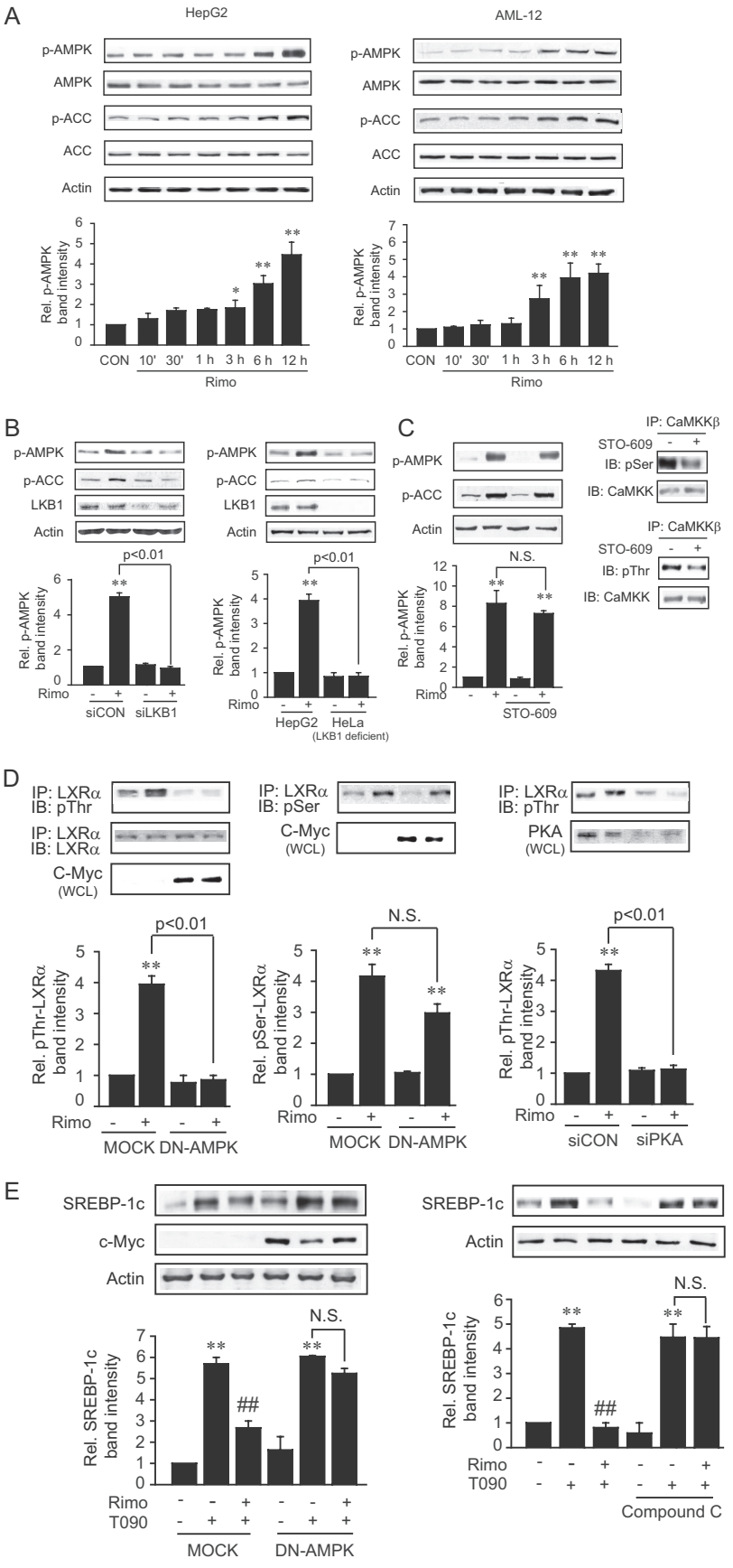

Fig. 6. LKB1 regulation of AMPK for the repression of LXRα and SREBP-1c. A, AMPK activation by rimonabant (Rimo). B, LKB1-dependent AMPK activation. HepG2 cells were treated with 10 μM rimonabant for 6 h after transfection of control siRNA or siRNA directed against LKB1 (100 pmol/ml, 48 h). HeLa cells were treated with 10 μM rimonabant for 6 h. C, effect of CaMKKβ inhibition on the activation of AMPK. Cells were treated with 1 μg/ml STO-609 for 30 min and were continuously incubated with 10 μM rimonabant for 6 h. Inset, immunoblots (IB) of CaMKK immunoprecipitates (IP) for phosphoserine or phosphothreonine confirmed the inhibition of CaMKK activity by STO-609. D, effect of DN-AMPK transfection or PKA knockdown (100 pmol/ml, 48 h) on LXRα phosphorylation by rimonabant. LXRα immunoprecipitates were immunoblotted with anti-phosphorylated threonine or anti-phosphorylated serine antibody. The LXRα control blot shown in D, left, is for pSer-LXRα (D, middle). The LXRα control blot shown in Fig. 4A, left, is for pThr-LXRα (D, right). Immunoblots for c-myc confirmed DN-AMPK overexpression. After verifying equal loading of proteins in each experiment by immunoblotting of LXRα immunoprecipitates for LXRα, the relative protein levels of pSer-LXRα or pThr-LXRα from at least three separate experiments were compared among four treatment groups in each experimental set (i.e., MOCK + vehicle, MOCK + rimonabant, DN-AMPK + vehicle, and DN-AMPK + rimonabant; or siCON + vehicle, siCON + rimonabant, siPKA+vehicle, and siPKA + rimonabant) by analysis of variance and multiple comparisons. E, effects of AMPK inhibition on SREBP-1c repression by rimonabant. Immunoblots for SREBP-1c were performed on the lysates of HepG2 cells treated with 1 μM T090 or 1 μM T090 plus 10 μM rimonabant for 12 h after DN AMPK transfection or 5 μM compound C treatment. For all immunoblots, data represent the mean $\pm$ S.E. for at least three separate experiments. The statistical significance of differences between each treatment group and control ($*$, $p < 0.05$; $**$, $p < 0.01$) or T090 alone (##, $p < 0.01$) was determined. Rel., relative; CON, control; p, phosphorylated; siCON, control siRNA; siPKA, PKA siRNA; siLKB1, LKB1 siRNA; N.S., not significant.

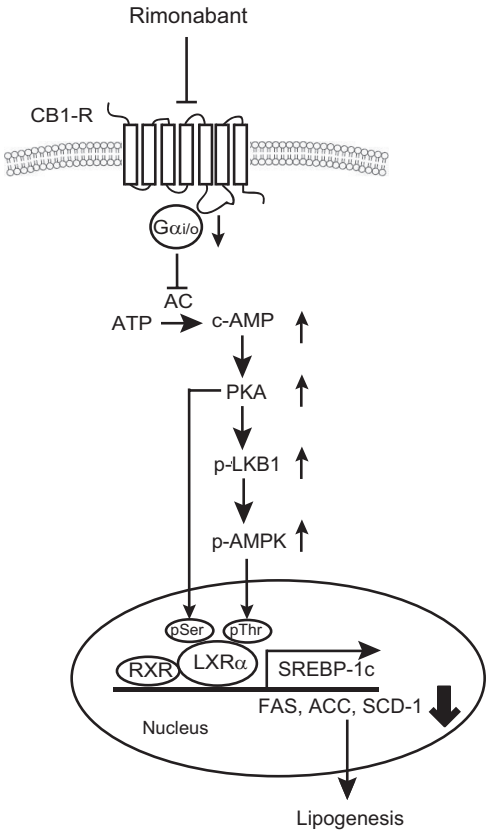

Fig. 7. A schematic diagram illustrating the proposed mechanism by which rimonabant inhibits LXRα-SREBP-1c-mediated steatosis in hepatocytes. RXR, retinoid X receptor.

weight loss effect as well as metabolic syndrome correction (Després et al., 2005). Unfortunately, it was recently withdrawn from the market because of neuropsychiatric adverse events (Nathan et al., 2010). Nevertheless, the endocannabinoid system still has an important research value in new drug development because peripheral CB1 antagonism shows a potential beneficial effect in regulating metabolic syndrome. Because drugs with no psychiatric disturbances seem particularly interesting, one possible future aim is the development of endocannabinoid modulators that have only peripheral effects.

LXRα facilitates fatty acid synthesis mainly through transcription of SREBP-1c, a master regulator of lipogenic genes (Repa et al., 2000). The role of LXRα in lipogenesis was proven by the result of an in vivo experiment showing that administration of an LXR agonist (T090) to mice increased hepatic and plasma triglyceride levels and switched on LXR-dependent lipogenic genes in the liver, whereas this effect was abolished in LXR-null mice (Schultz et al., 2000). In the present study, we explored the mechanistic basis of the antilipogenic properties of rimonabant in a hepatocyte model using LXRα ligand. Our finding that the pharmacological interference on CB1 suppressed T090 induction of SREBP-1c expression is in agreement with the observation that treatment of HU 210, a CB1 agonist, enhanced the SREBP-1c level in mice, which was abolished by rimonabant pretreatment (Osei-Hyiaman et al., 2005). All these results support the notion that rimonabant may act peripherally in the liver to antagonize CB1 and decrease LXRα-dependent SREBP-1c induction, leading to reduced fatty acid synthesis. The lack of increase in the SREBP-1c level by HU 210 or ACEA treatment alone may be due to weak activity of the endogenous LXRα ligand (De Gottardi et al., 2010). Without LXRα ligand, CB1-mediated signal transduction might not be sufficient to activate LXRα. In addition, the CB1 agonist treatment did not potentiate the lipogenic effect of either 0.1 or 1 μM T090: this might result from limiting activity of downstream molecule(s).

CB1 belongs to the superfamily of GPCRs. Ligand activation of CB1 transmits signals to the G proteins of the $G\alpha_{i/o}$ family (Howlett et al., 1986). The agonist-stimulated CB1 signal transduction pathway results in the inhibition of adenylyl cyclase activity through $G\alpha_{i/o}$ proteins (Howlett et al., 1986). An important finding of the current study is the identification of $G\alpha_{i/o}$ inhibition, especially $G\alpha_{i}$ inhibition, as a modulating step that prevents LXRα-dependent steatosis. This hypothesis was strengthened by not only the repression of SREBP-1c after either $G\alpha_{i}$ knockdown or chemical inhibition of $G\alpha_{i/o}$ but also the reversal of rimonabant's effect by a CB1 agonist that stimulates $G\alpha_{i/o}$ (Glass and Northup, 1999).

Inhibition of adenylyl cyclase by $G\alpha_{i/o}$ activation decreases cellular cAMP content in most tissues and cells (Neves et al., 2002). On the contrary, an increase in cAMP content by $G\alpha_{i/o}$ inhibition contributed to the antilipogenic effect of rimonabant in the present study, as supported by SREBP-1c repression after forskolin or 8-Br-cAMP treatment. It is well recognized that cAMP activates PKA, a major protein kinase involved in energy metabolic pathways (e.g., lipid metabolism). As expected, our data shown here demonstrated the bona fide activation of PKA after rimonabant treatment, which agrees with the reports shown in the experiments using muscle or endothelial cells (Esposito et al., 2008; Huang et al., 2010). PKA directly phosphorylates LXRα at the serine residue and impairs LXRα-DNA binding by inhibiting LXRα and retinoid X receptor dimerization. Thus, PKA activation suppresses SREBP-1c induction by LXRα both in vitro and in vivo (Yamamoto et al., 2007). An important aspect of our finding is the identification of rimonabant's activation of PKA for the inhibition of LXRα-mediated SREBP-1c induction. This concept was also strengthened by our observation that rimonabant enhanced LXRα serine phosphorylation through PKA.

LKB1 activates several kinases in the cell (Hawley et al., 2003). Another novel finding of our study is the activation of LKB1 by rimonabant, as supported by our finding that rimonabant treatment decreased lysine acetylation of LKB1 with an increase in its CAB39 binding. SIRT1 regulates LKB1 deacetylation and thereby promotes its translocation to the cytoplasm and binding with STRAD and CAB39 (Boudeau et al., 2003; Lan et al., 2008). This complex formation then enhances the catalytic activity of LKB1. PKA is known as an upstream kinase of LKB1 (Sapkota et al., 2001). Our results also provided evidence that a deficiency in PKA prevented LKB1 activation by rimonabant, corroborating the regulatory effect of PKA on LKB1. Poly(ADP-ribose) polymerase is another possible regulator of LKB1 (Shin et al., 2009). In an additional experiment, we found that rimonabant failed to change the level of poly(ADP-ribose) polymerase (data not shown). Hence, it is highly likely that PKA activation by rimonabant contributes to LKB1 activation.

LKB1 and CaMKK are the two main upstream kinases of AMPK (Hawley et al., 2003, 2005). LKB1-dependent AMPK

activation by a natural product, ajoene, contributed to treating high-fat diet-induced hepatic steatosis (Han et al., 2011). The present finding also showed that LKB1 was necessary for the activation of AMPK by rimonabant, which was verified by the reversal of this effect by LKB1 knockdown. AMPK plays a role in lipid metabolism; it reduces fatty acid synthesis by down-regulating SREBP-1c and its target genes (Zhou et al., 2001). Cannabinoids that activate CB1 inhibited the activity of AMPK in the liver and stimulated lipogenic and diabetogenic effects (Kola et al., 2005). In an *ob/ob* mouse model, rimonabant increased hepatic AMPK activity and enhanced the synthesis of adiponectin, a hormone that possibly activates AMPK (Watanabe et al., 2009). Hwahng et al. (2009) showed an opposite role of AMPK and p70 ribosomal S6 kinase-1 (S6K1) in regulating LXRα activity: the inhibitory and activating phosphorylation of LXRα was mediated by AMPK and S6K1, respectively. The role of AMPK in SREBP-1c repression by rimonabant was confirmed by our finding that AMPK inhibition reversed the repressing effect of rimonabant on LXRα and SREBP-1c. However, overexpression of an activated mutant of S6K1 did not affected it (data not shown), suggesting that the antilipogenic effect of rimonabant may stem from LKB1-dependent AMPK activation but not S6K1 inhibition.

In our study, PKA was activated at an early time (i.e., 30 min), which may also be directly responsible for rimonabant's antilipogenic effect via the inhibitory phosphorylation of LXRα at serine (i.e., two consensus PKA target sites at serine 195/196 and serine 290/291). PKA activation by isoproterenol leads to AMPK phosphorylation at Ser173 at an early phase (0.5–2 h), and delayed AMPK phosphorylation at Thr172 (Djouder et al., 2010). The phosphorylation of AMPK at Ser173 by PKA precludes AMPK phosphorylation at Thr172 by LKB1 at an early phase. We found that AMPK phosphorylation occurred at later times (3–12 h) after activating phosphorylation of LKB1 (0.5–12 h) after rimonabant treatment. AMPK directly phosphorylates LXRα at the threonine residue and thereby inhibits LXRα activity (Hwahng et al., 2009). Thus, inhibition of lipogenesis by rimonabant at an early phase may be directly controlled by PKA, whereas that at the later phase may be controlled by AMPK downstream of the PKA-LKB1 axis. Overall, our finding indicates that the antilipogenic effect of rimonabant in hepatocytes may rely on the activation of PKA, a kinase that on the one hand directly inhibits LXRα via serine phosphorylation and on the other hand stimulates LKB1 for AMPK activation; the activated AMPK would then inhibit LXRα for a prolonged period of time through threonine phosphorylation.

In conclusion, we found that rimonabant has the ability to inhibit lipogenesis in hepatocytes, which may result from inhibition of LXRα-dependent SREBP-1c induction, as mediated by LKB1-AMPK activation downstream of the CB1-coupled G$\alpha_{i/o}$-PKA axis (Fig. 7). Collectively, the results of the current study bring additional information on the pharmacology and mechanistic basis of the CB1 inverse agonist, providing insight in determining the use of CB1 antagonism for steatosis in hepatocytes.

Authorship Contributions

Participated in research design: Wu, Yang, and Kim.
Conducted experiments: Wu and Yang.
Performed data analysis: Wu, Yang, and Kim.
Wrote or contributed to the writing of the manuscript: Wu, Yang, and Kim.

References

Alexander CM, Landsman PB, Teutsch SM, Haffner SM, Third National Health and Nutrition Examination Survey (NHANES III), and National Cholesterol Education Program (NCEP) (2003) NCEP-defined metabolic syndrome, diabetes, and prevalence of coronary heart disease among NHANES III participants age 50 years and older. *Diabetes* **52:**1210–1214.

Bae EJ, Yang YM, Kim JW, and Kim SG (2007) Identification of a novel class of dithiolethiones that prevent hepatic insulin resistance via the adenosine monophosphate-activated protein kinase-p70 ribosomal S6 kinase-1 pathway. *Hepatology* **46:**730–739.

Bayewitch M, Avidor-Reiss T, Levy R, Barg J, Mechoulam R, and Vogel Z (1995) The peripheral cannabinoid receptor: adenylate cyclase inhibition and G protein coupling. *FEBS Lett* **375:**143–147.

Boudeau J, Baas AF, Deak M, Morrice NA, Kieloch A, Schutkowski M, Prescott AR, Clevers HC, and Alessi DR (2003) MO25α/β interact with STRADα/β enhancing their ability to bind, activate and localize LKB1 in the cytoplasm. *EMBO J* **22:**5102–5114.

Collins SP, Reoma JL, Gamm DM, and Uhler MD (2000) LKB1, a novel serine/threonine protein kinase and potential tumour suppressor, is phosphorylated by cAMP-dependent protein kinase (PKA) and prenylated in vivo. *Biochem J* **345:**673–680.

Cornier MA, Dabelea D, Hernandez TL, Lindstrom RC, Steig AJ, Stob NR, Van Pelt RE, Wang H, and Eckel RH (2008) The metabolic syndrome. *Endocr Rev* **29:**777–822.

Cummings DE, Brandon EP, Planas JV, Motamed K, Idzerda RL, and McKnight GS (1996) Genetically lean mice result from targeted disruption of the RII β subunit of protein kinase A. *Nature* **382:**622–626.

De Gottardi A, Spahr L, Ravier-Dall'Antonia F, and Hadengue A (2010) Cannabinoid receptor 1 and 2 agonists increase lipid accumulation in hepatocytes. *Liver Int* **30:**1482–1489.

Després JP, Golay A, Sjöström L, and Rimonabant in Obesity-Lipids Study Group (2005) Effects of rimonabant on metabolic risk factors in overweight patients with dyslipidemia. *N Engl J Med* **353:**2121–2134.

Djouder N, Tuerk RD, Suter M, Salvioni P, Thali RF, Scholz R, Vaahtomeri K, Auchli Y, Rechsteiner H, Brunisholz RA, et al. (2010) PKA phosphorylates and inactivates AMPKα to promote efficient lipolysis. *EMBO J* **29:**469–481.

Esposito I, Proto MC, Gazzerro P, Laezza C, Miele C, Alberobello AT, D'Esposito V, Beguinot F, Formisano P, and Bifulco M (2008) The cannabinoid CB1 receptor antagonist rimonabant stimulates 2-deoxyglucose uptake in skeletal muscle cells by regulating the expression of phosphatidylinositol-3-kinase. *Mol Pharmacol* **74:**1678–1686.

Glass M and Northup JK (1999) Agonist selective regulation of G proteins by cannabinoid CB_1 and CB_2 receptors. *Mol Pharmacol* **56:**1362–1369.

Han CY, Ki SH, Kim YW, Noh K, Lee da Y, Kang B, Ryu JH, Jeon R, Kim EH, Hwang SJ, et al. (2011) Ajoene, a stable garlic by-product, inhibits high fat diet-induced hepatic steatosis and oxidative injury through LKB1-dependent AMPK activation. *Antioxid Redox Signal* **14:**187–202.

Hawley SA, Boudeau J, Reid JL, Mustard KJ, Udd L, Mäkelä TP, Alessi DR, and Hardie DG (2003) Complexes between the LKB1 tumor suppressor, STRAD alpha/beta and MO25α/β are upstream kinases in the AMP-activated protein kinase cascade. *J Biol* **2:**28.

Hawley SA, Pan DA, Mustard KJ, Ross L, Bain J, Edelman AM, Frenguelli BG, and Hardie DG (2005) Calmodulin-dependent protein kinase kinase-β is an alternative upstream kinase for AMP-activated protein kinase. *Cell Metab* **2:**9–19.

Hollander PA, Amod A, Litwak LE, Chaudhari U, and ARPEGGIO Study Group (2010) Effect of rimonabant on glycemic control in insulin-treated type 2 diabetes: the ARPEGGIO trial. *Diabetes Care* **33:**605–607.

Howlett AC, Qualy JM, and Khachatrian LL (1986) Involvement of G_i in the inhibition of adenylate cyclase by cannabimimetic drugs. *Mol Pharmacol* **29:**307–313.

Huang NL, Juang JM, Wang YH, Hsueh CH, Liang YJ, Lin JL, Tsai CT, and Lai LP (2010) Rimonabant inhibits TNF-α-induced endothelial IL-6 secretion via CB1 receptor and cAMP-dependent protein kinase pathway. *Acta Pharmacol Sin* **31:**1447–1453.

Hwahng SH, Ki SH, Bae EJ, Kim HE, and Kim SG (2009) Role of adenosine monophosphate-activated protein kinase-p70 ribosomal S6 kinase-1 pathway in repression of liver X receptor-α-dependent lipogenic gene induction and hepatic steatosis by a novel class of dithiolethiones. *Hepatology* **49:**1913–1925.

Jeong WI, Osei-Hyiaman D, Park O, Liu J, Bátkai S, Mukhopadhyay P, Horiguchi N, Harvey-White J, Marsicano G, Lutz B, et al. (2008) Paracrine activation of hepatic CB1 receptors by stellate cell-derived endocannabinoids mediates alcoholic fatty liver. *Cell Metab* **7:**227–235.

Jourdan T, Djaouti L, Demizieux L, Gresti J, Vergès B, and Degrace P (2010) CB1 antagonism exerts specific molecular effects on visceral and subcutaneous fat and reverses liver steatosis in diet-induced obese mice. *Diabetes* **59:**926–934.

Kola B, Hubina E, Tucci SA, Kirkham TC, Garcia EA, Mitchell SE, Williams LM, Hawley SA, Hardie DG, Grossman AB, et al. (2005) Cannabinoids and ghrelin have both central and peripheral metabolic and cardiac effects via AMP-activated protein kinase. *J Biol Chem* **280:**25196–25201.

Kotronen A and Yki-Järvinen H (2008) Fatty liver: a novel component of the metabolic syndrome. *Arterioscler Thromb Vasc Biol* **28:**27–38.

Laffitte BA, Joseph SB, Walczak R, Pei L, Wilpitz DC, Collins JL, and Tontonoz P (2001) Autoregulation of the human liver X receptor α promoter. *Mol Cell Biol* **21:**7558–7568.

Lan F, Cacicedo JM, Ruderman N, and Ido Y (2008) SIRT1 modulation of the

acetylation status, cytosolic localization, and activity of LKB1. Possible role in AMP-activated protein kinase activation. *J Biol Chem* **283:**27628–27635.
Liu YL, Connoley IP, Wilson CA, and Stock MJ (2005) Effects of the cannabinoid CB1 receptor antagonist SR141716 on oxygen consumption and soleus muscle glucose uptake in *Lep*^{ob}/*Lep*^{ob} mice. *Int J Obes* (*Lond*) **29:**183–187.
Lu M and Shyy JY (2006) Sterol regulatory element-binding protein 1 is negatively modulated by PKA phosphorylation. *Am J Physiol Cell Physiol* **290:**C1477–C1486.
Marra F, Gastaldelli A, Svegliati Baroni G, Tell G, and Tiribelli C (2008) Molecular basis and mechanisms of progression of non-alcoholic steatohepatitis. *Trends Mol Med* **14:**72–81.
McKnight GS, Cummings DE, Amieux PS, Sikorski MA, Brandon EP, Planas JV, Motamed K, and Idzerda RL (1998) Cyclic AMP, PKA, and the physiological regulation of adiposity. *Recent Prog Horm Res* **53:**139–159; discussion 160–161.
Mitro N, Vargas L, Romeo R, Koder A, and Saez E (2007) T0901317 is a potent PXR ligand: implications for the biology ascribed to LXR. *FEBS Lett* **581:**1721–1726.
Motoshima H, Goldstein BJ, Igata M, and Araki E (2006) AMPK and cell proliferation—AMPK as a therapeutic target for atherosclerosis and cancer. *J Physiol* **574:**63–71.
Nathan PJ, O'Neill BV, Napolitano A, and Bullmore ET (2010) Neuropsychiatric adverse effects of centrally acting antiobesity drugs. *CNS Neurosci Ther* doi: 10.1111/j.1755–5949.2010.00172.x.
Neves SR, Ram PT, and Iyengar R (2002) G protein pathways. *Science* **296:**1636–1639.
Ntambi JM (1999) Regulation of stearoyl-CoA desaturase by polyunsaturated fatty acids and cholesterol. *J Lipid Res* **40:**1549–1558.
Osei-Hyiaman D, DePetrillo M, Pacher P, Liu J, Radaeva S, Bátkai S, Harvey-White J, Mackie K, Offertáler L, Wang L, et al. (2005) Endocannabinoid activation at hepatic CB1 receptors stimulates fatty acid synthesis and contributes to diet-induced obesity. *J Clin Invest* **115:**1298–1305.
Repa JJ, Liang G, Ou J, Bashmakov Y, Lobaccaro JM, Shimomura I, Shan B, Brown MS, Goldstein JL, and Mangelsdorf DJ (2000) Regulation of mouse sterol regulatory element-binding protein-1c gene (SREBP-1c) by oxysterol receptors, LXRα and LXRβ. *Genes Dev* **14:**2819–2830.
Sakoda H, Ogihara T, Anai M, Fujishiro M, Ono H, Onishi Y, Katagiri H, Abe M, Fukushima Y, Shojima N, et al. (2002) Activation of AMPK is essential for AICAR-induced glucose uptake by skeletal muscle but not adipocytes. *Am J Physiol Endocrinol Metab* **282:**E1239–E1244.
Sapkota GP, Kieloch A, Lizcano JM, Lain S, Arthur JS, Williams MR, Morrice N, Deak M, and Alessi DR (2001) Phosphorylation of the protein kinase mutated in Peutz-Jeghers cancer syndrome, LKB1/STK11, at Ser^{431} by p90^{RSK} and cAMP-dependent protein kinase, but not its farnesylation at Cys^{433}, is essential for LKB1 to suppress cell growth. *J Biol Chem* **276:**19469–19482.
Scheen AJ, Finer N, Hollander P, Jensen MD, Van Gaal LF, and RIO-Diabetes Study Group (2006) Efficacy and tolerability of rimonabant in overweight or obese patients with type 2 diabetes: a randomised controlled study. *Lancet* **368:**1660–1672.
Schreyer SA, Cummings DE, McKnight GS, and LeBoeuf RC (2001) Mutation of the RIIβ subunit of protein kinase A prevents diet-induced insulin resistance and dyslipidemia in mice. *Diabetes* **50:**2555–2562.
Schultz JR, Tu H, Luk A, Repa JJ, Medina JC, Li L, Schwendner S, Wang S, Thoolen M, Mangelsdorf DJ, et al. (2000) Role of LXRs in control of lipogenesis. *Genes Dev* **14:**2831–2838.
Shin SM, Cho IJ, and Kim SG (2009) Resveratrol protects mitochondria against oxidative stress through AMP-activated protein kinase-mediated glycogen synthase kinase-3 inhibition downstream of poly(ADP-ribose)polymerase-LKB1 pathway. *Mol Pharmacol* **76:**884–895.
Stoeckman AK and Towle HC (2002) The role of SREBP-1c in nutritional regulation of lipogenic enzyme gene expression. *J Biol Chem* **277:**27029–27035.
Van Gaal LF, Rissanen AM, Scheen AJ, Ziegler O, Rössner S, and RIO-Europe Study Group (2005) Effects of the cannabinoid-1 receptor blocker rimonabant on weight reduction and cardiovascular risk factors in overweight patients: 1-year experience from the RIO-Europe study. *Lancet* **365:**1389–1397.
Watanabe T, Kubota N, Ohsugi M, Kubota T, Takamoto I, Iwabu M, Awazawa M, Katsuyama H, Hasegawa C, Tokuyama K, et al. (2009) Rimonabant ameliorates insulin resistance via both adiponectin-dependent and adiponectin-independent pathways. *J Biol Chem* **284:**1803–1812.
Yamamoto T, Shimano H, Inoue N, Nakagawa Y, Matsuzaka T, Takahashi A, Yahagi N, Sone H, Suzuki H, Toyoshima H, et al. (2007) Protein kinase A suppresses sterol regulatory element-binding protein-1C expression via phosphorylation of liver X receptor in the liver. *J Biol Chem* **282:**11687–11695.
Yan ZC, Liu DY, Zhang LL, Shen CY, Ma QL, Cao TB, Wang LJ, Nie H, Zidek W, Tepel M, et al. (2007) Exercise reduces adipose tissue via cannabinoid receptor type 1 which is regulated by peroxisome proliferator-activated receptor-delta. *Biochem Biophys Res Commun* **354:**427–433.
Zhou G, Myers R, Li Y, Chen Y, Shen X, Fenyk-Melody J, Wu M, Ventre J, Doebber T, Fujii N, et al. (2001) Role of AMP-activated protein kinase in mechanism of metformin action. *J Clin Invest* **108:**1167–1174.

Address correspondence to: Dr. Sang Geon Kim, College of Pharmacy, Seoul National University, Sillim-dong, Kwanak-gu, Seoul 151-742, Korea. E-mail: sgk@snu.ac.kr

Correction to "Rimonabant, a Cannabinoid Receptor Type 1 Inverse Agonist, Inhibits Hepatocyte Lipogenesis by Activating Liver Kinase B1 and AMP-Activated Protein Kinase Axis Downstream of $G\alpha_{i/o}$ Inhibition"

In the above article [Wu HM, Yang, YM, and Kim SG (2011) *Mol Pharmacol* **80:**859–869], several figures contained errors that require correction and explanation.

The IP/IB Western blots shown in Figs. 4A, left, and 6D, right, were done using the same LXRα immunoprecipitates; likewise, those in 6D, left and middle, were done using the same LXRα immunoprecipitates. However, the first lane of the LXRα band in Fig. 4A, right, was accidentally overlapped with the fourth lane of the LXRα band in Fig. 6D, left. Corrected versions of Figs. 4A and 6D, along with the related raw blots and corrected legends, are provided below.

In addition, two lanes loaded for positive control were mistakenly included in the p-ACC band in Fig. 6A, right. The corrected band and the related raw blot are provided below.

Finally, in the scheme in Fig. 7, "AMP" should be "ATP."

The online version of this article has been updated in departure from the print version.

The authors regret these errors and apologize for any confusion or inconvenience they may have caused.

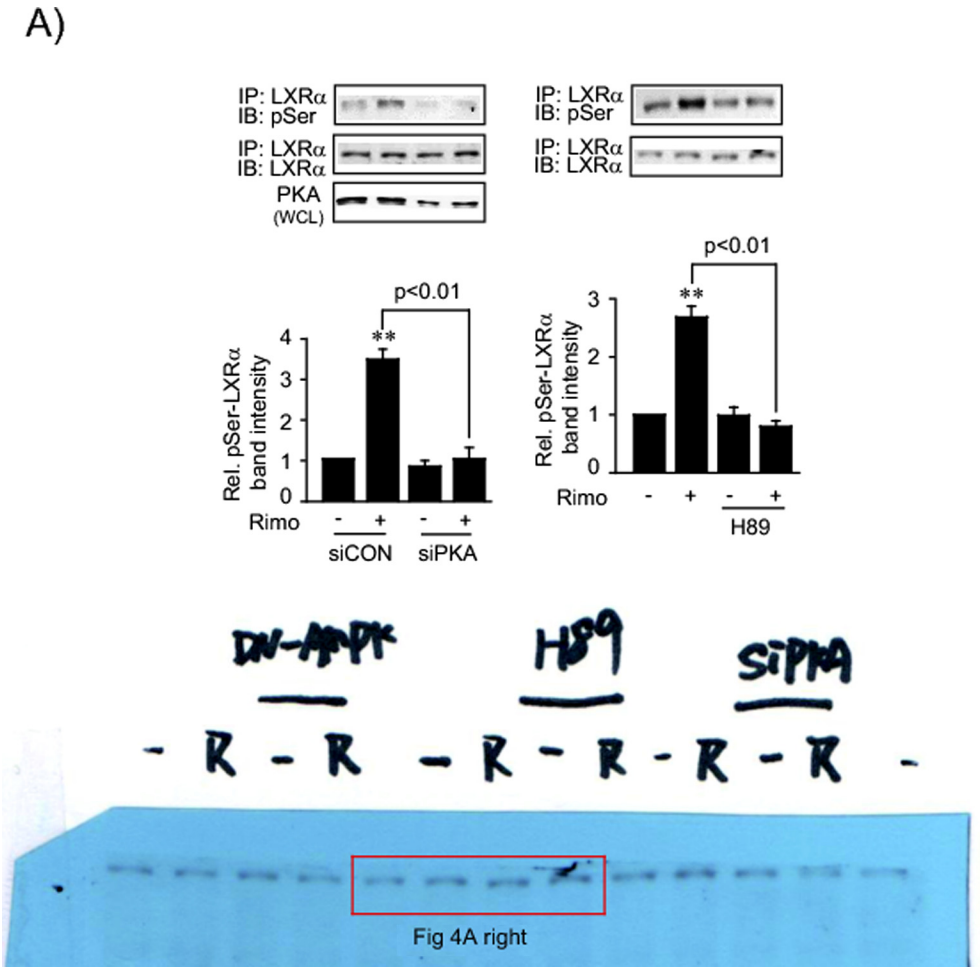

Fig. 4. A, effect of PKA on serine phosphorylation of LXRα by rimonabant. HepG2 cells were treated with vehicle or 10 μM rimonabant after siPKA transfection (100 pmol/ml) for 48 h or 1 μM H89 treatment for 1 h. LXRα immunoprecipitates (IP) were immunoblotted (IB) with anti-phosphorylated serine antibody (pSer). After verifying equal loading of proteins in each experiment by immunoblotting of LXRα immunoprecipitates for LXRα, the relative protein levels of pSer-LXRα from at least three separate experiments were compared among four treatment groups in each experimental set (i.e., siCON + vehicle, siCON + rimonabant, siPKA + vehicle, and siPKA + rimonabant, or vehicle, vehicle + rimonabant, H89 + vehicle, and H89 + rimonabant) by analysis of variance and multiple comparisons (**, $p < 0.01$; compared from siCON + vehicle or vehicle-treated group). Left LXRα control blot is also the control blot for pThr-LXRα (Fig 6D, right). WCL, whole cell lysate. (Legend continues as in original.)

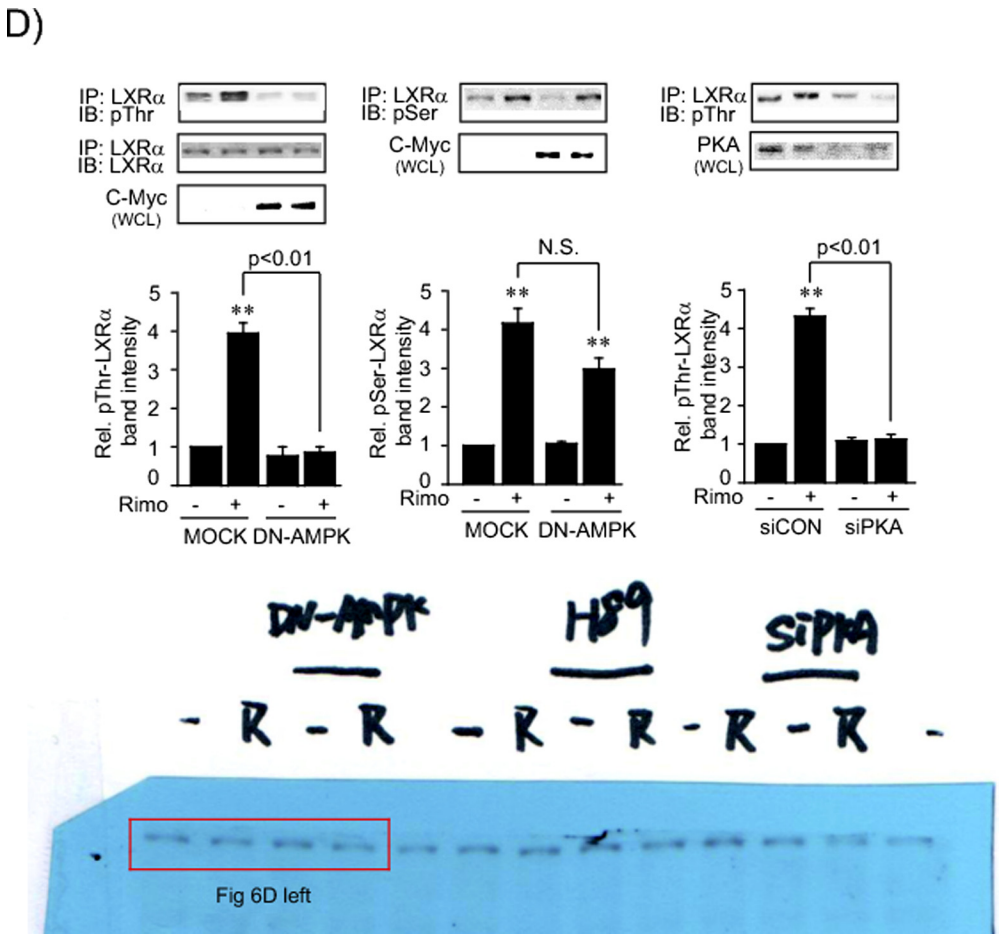

Fig. 6. (Legend begins as in original.) D, effect of DN-AMPK transfection or PKA knockdown (100 pmol/ml, 48 h) on LXRα phosphorylation by rimonabant. LXRα immunoprecipitates (IP) were immunoblotted (IB) with anti-phosphorylated threonine (pThr) or anti-phosphorylated serine (pSer) antibody. The LXRα control blot shown in D, left, is for pSer-LXRα (D, middle). The LXRα control blot shown in Fig. 4A, left, is for pThr-LXRα (D, right). Immunoblots for c-*myc* confirmed DN-AMPK overexpression. After verifying equal loading of proteins in each experiment by immunoblotting of LXRα immunoprecipitates for LXRα, the relative protein levels of pSer-LXRα or pThr-LXRα from at least three separate experiments were compared among four treatment groups in each experimental set (i.e., MOCK + vehicle, MOCK + rimonabant, DN-AMPK + vehicle, and DN-AMPK + rimonabant; or siCON + vehicle, siCON + rimonabant, siPKA + vehicle, and siPKA + rimonabant) by analysis of variance and multiple comparisons.

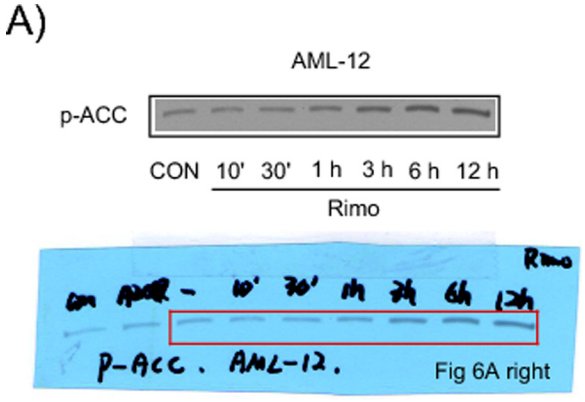

Fig. 6A. A, AMPK activation by rimonabant (Rimo).